Table 1 Suppressive effect of the A120 mAb on various clades of HIV-1 strains.

Member	HIV-1 Subtype	Isolate	Country of Origin	Syncytium	Co-receptor Usage	Percent inhibition of p24 production
PRD320-01	A	UG275	Uganda	NSI	CCR5	88.3%
PRD320-02	A	I-2496	Ghana	NSI	CCR5	99.8%
PRD320-03	CRF02_AG	DJ263	Djibouti	NSI	CCR5	94.7%
PRD320-04	CRF02_AG	POC44951	Liberia	NSI	CCR5	99.7%
PRD320-06	B	BZ167	Brazil	SI	CXCR4	97.2%
PRD3200-7	C	DJ259	Djibouti	NSI	CCR5	91.5%
PRD320-08	C	ZAM18	Zambia	NSI	CCR5	93.7%
PRD320-09	D	SE365	Senegal	SI	CXCR4	98.5%
PRD320-10	D	UG270	Uganda	SI	CXCR4	99.7%
PRD320-11	CRF01_AE	ID17	Indonesia	NSI	CCR5	81.0%
PRD320-12	CRF01_AE	NP03	Thailand	SI	CXCR4	94.5%
PRD320-14	F	BCI-R07	Romania	SI	CXCR4/CCR5	99.4%
PRD320-15	G	BCF-DIOUM	Zaire	NSI	CCR5	99.9%
PRD320-16	G	HH8793	Kenya	NSI	CCR5	83.3%
PRD320-17	H	BCF-KITA	Zaire	NSI	CCR5	92.5%
PRD320-18	O	BCF06	Cameroon	SI	CXCR4/CCR5	98.3%
PRD320-19	O	I-2478B	US	NSI	CCR5	65.6%

Anti-CD3/CD28 activated PBMCs were infected with each of 15 different HIV-1 strains belonging to various clades and with previously defined different CXCR4 and CCR5 usages. HIV-1 dose of 10 ng p24 value was added to 1 × 10^6 cells for infection. After washing, PBMCs were aliquoted and cultured in triplicate in the presence of 10 μg/ml of the A120 mAb or isotype control IgG for 5 days. Virus production was determined by quantitation of p24 in the culture supernatants by ELISA and the mean values calculated. Percent inhibition was calculated relative to the values obtained with the isotype control mAb alone. Representative data from three independent experiments are shown.

So far, similar suppression of both X4 and R5 HIV-1 infection has also been reported in a study utilizing anti-human CCR2 mAb that is neither agonistic nor antagonistic [14]. It was reasoned that this anti-CCR2 mAb functions by the induction of hetero-oligomerization of CCR2 with CCR5 and CXCR4, but not receptor down-modulation. Another report showed that a non-agonistic/antagonistic anti-CCR5 N-terminus specific mAb that is unable to block the binding of R5 HIV-1 gp120 to CCR5 interferes with R5 HIV-1 infection by induction of CCR5 dimerization rather than down-modulation of CCR5 [16]. It is of interest to note that this anti-CCR5 mAb does not inhibit X4 HIV-1. Thus, our finding that ligation of CXCR4 via the ECL1/ECL2 region on activated PBMCs results in the production of CCR5-binding β-chemokines followed by down-modulation of CCR5 expression is unique. However, it remains to be determined whether the ligation of CXCR4 with the A120 mAb similarly induces hetero-dimerization of CXCR4 with CCR5 or the other chemokine receptors or CCR5 homo-dimerization. Further studies are in progress using immunoprecipitation and Western blot techniques utilizing appropriate mAbs.

It is important to note that the addition of anti-chemokine mAbs did not show the same degree of reversal of the A120 mAb-induced inhibition of R5 HIV-1 infection in the cultures from 2 out of the 6 PBMC donors (Figure 6). In addition, there was a lack of correlation between enhanced β-chemokine levels and the reversing effects of the anti-β-chemokine antibodies on the A120-mediated R5 HIV-1 inhibition. We assume that the concentration of the β-chemokine antibodies (10 μg/ml) was sufficient to neutralize endogenously produced β-chemokines as the antibodies at this concentration could neutralize > 100 ng/ml of each of the recombinant β-chemokines (data not shown). While resistance of these donors was not due to the production of some other anti-HIV-1 factor such as $CD8^+$T lymphocyte antiviral factor (CAF) [17], it may be possible that treatment with the A120 mAb might induce the hetero-dimerization of CXCR4 and CCR5 which results in resistance to R5 HIV-1 infection. Further studies are in progress to address this issue. It is interesting to note that among the neutralizing mAbs against the β-chemokines, the anti-MIP-1α mAb was the most effective in reversing the A120 mAb-induced R5 HIV-1 inhibition. Since all the available anti-MIP-1α mAbs at present do not distinguish MIP-1α (LD78α) from its homologue CCR3L1 product (LD78β) [18], it is possible that CCR3L1 protein is also produced upon A120 mAb treatment and involved in the R5 HIV-1 inhibition. As CCR3L1 is known to be a potent factor that may delay the progression to clinical AIDS [19], it will be important to determine whether A120 mAb stimulates the production of CCR3L1 proteins. Such studies are also in progress.

The generation of resistance to CCR5 inhibitors involving either the selection of pre-existing CXCR4 tropic HIV-1 and/or due to the evolution of Env variants has been well documented [20]. Thus, in such cases, the availability of a reagent like the A120 mAb that has inhibitory properties for both CCR5 and CXCR4 tropic HIV-1 may provide a unique therapeutic tool worthy of consideration. Since the A120 mAb also inhibits the SIV-1 infection in activated PBMCs from rhesus macaques (Takahashi et al., unpublished), this hypothesis is currently being investigated using the nonhuman primate model.

Conclusions

Data described herein have identified a unique epitope of CXCR4 whose ligation not only directly inhibits CXCR4 tropic HIV-1, but also indirectly inhibits the infection of R5 tropic HIV-1 via the synthesis of natural CCR5 ligands.

Methods

Reagents

RPMI 1640 medium (Sigma-Aldrich. Inc. St. Louis, MO) supplemented with 10% fetal calf serum (FCS), 100 U/ml of penicillin and 100 μg/ml of streptomycin (hereinafter called RPMI medium) was utilized for the described studies. Anti-human CD3 (clone OKT-3) and anti-CD28 (clone 28.2) were obtained from the American Type Culture Collection (Rockville, MD) and BioLegend (San Diego, CA), respectively. Neutralizing mAbs against human RANTES, MIP-1α and MIP-1β were purchased from R&D systems (Minneapolis, MN). The rat anti-CXCR4 mAbs used were produced in our laboratory and included clones A145 (IgG1), A120 (IgG2b) and A80 (IgG1) [16]. Mapping of the epitopes recognized by these mAbs was reported previously [16]. Other rat mAbs used were IgG1 anti-CCR5, IgG2b anti-HTLV-I gp46 and IgG1 anti-HCV produced in our laboratory [16,21,22]. These mAbs were purified from CB.17-SCID mouse ascites fluids by ammonium sulfate precipitation followed by gel filtration using Superdex G-200 (GE), and passed through a polymyxin B column to remove potential LPS contamination. The fluorescent dye-labeled anti-human CD4, CD8, CD14 and CD19 mAbs were purchased from Beckman-Coulter or BioLegend. The anti-HIV-1 p24 mAbs used were also produced in our laboratory. Magnetic beads conjugated with mAbs against human CD4, CD8, CD14 or CD19 were purchased from Dynal and used according to the manufacturer's recommendation. Low endotoxin murine anti-CXCR4 mAbs including clone 12G5 and the other anti-CXCR4 ECL2 mAbs were purchased from BioLegend and R&D.

HIV-1 preparation

Virus stocks of R5 HIV-1_{JR-FL}, R5 HIV-1_{JR-CSF} and X4 HIV-1_{NL4-3} were produced by transfection of the 293T cells with the appropriate HIV-1 infectious plasmid DNAs utilizing the calcium phosphate method as described previously [23]. X4 HIV-1_{IIIB} was produced in the Molt-4/IIIB cell line. The other HIV-1 isolates used were from the HIV subtype infectivity panel PRD320 (BBI Diagnostics, West Bridgewater, MA, USA) which included clade A R5 HIV-1 (UG275, I-2496 isolates), clade CRF02AG R5 HIV-1 (DJ263, POC44951 isolates), clade B R5 (US2 isolate) and X4 HIV-1 (BZ167 isolate), clade C R5 HIV-1 (DJ259, ZAM18 isolates), clade D X4 HIV-1 (SE365, UG270 isolates), clade CRF01AE R5 (ID17 isolate) and X4 HIV-1 (NP03 isolate), clade F R5 (BZ163 isolate) and X4/R5 HIV-1 (BCI-R17 isolate), clade G R5 HIV-1 (BCF-DIOUM, HH8793 isolates), clade H R5 HIV-1 (BCF-KITA isolate), clade O R5 (I-2478B isolate) and X4/R5 HIV-1(BCF06 isolate). Each of these panel HIV-1 strains was grown in primary PHA-activated PBMCs and the levels of p24 determined and 10 ng of p24 used to infect PBMCs. These HIV-1 stocks were aliquoted and stored at -80°C until used.

In vitro stimulation of PBMCs and infection with HIV-1

PBMCs from healthy donors were obtained by density gradient centrifugation on HistoPAQUE-1077 (Sigma-Aldrich), suspended at 2×10^6 cells/ml in RPMI medium, dispensed into individual wells of 24-well plates (BD) (1 ml/well) pre-coated with 5 μg/ml anti-CD3 mAb (OKT-3) and cultured in the presence of soluble 0.1 μg/ml anti-CD28 mAb at 37°C in a 5% CO_2 humidified atmosphere for 24 hours. The activated PBMCs were collected, washed once and infected with HIV-1 at a multiplicity of infection (m.o.i.) of 0.005~0.01 or at 10 ng p24 per $1\sim2 \times 10^6$ cells for 2 hours. Infected PBMCs were washed three times, re-suspended at $0.5\sim1 \times 10^6$ cells/ml in RPMI medium containing 20 U/ml recombinant human IL-2 containing RPMI medium, dispensed into individual wells of 48-well plates (BD) (0.5 ml/well) and then cultured in the presence or absence of various concentrations of the anti-CXCR4 or control mAbs. Production of HIV-1 was determined by the measurement of HIV-1 core p24 levels by ELISA, and the number of HIV-1 $p24^+$ cells were determined by FCM as described previously [24]. For select experiments, activated PBMCs were cultured at 1×10^6 cells/ml in RPMI medium containing 20 U/ml IL-2 in the presence or absence of 10 μg/ml of A120 mAb for 24 hours, and the culture supernatants were collected, and the levels of β-chemokines were determined by ELISA. All the experiments in this study were performed in triplicate wells.

Cell lines

Molt-4/IIIB [25] and MT-2 [26] cells that were productively infected with HIV-1IIIB (Molt-4/IIIB) and human T cell leukemia virus type-I (HTLV-I), respectively, were cultured in RPMI medium. HIV-1 and HTLV-I production were determined by our in-house HIV-1 p24 and HTLV-I p24 sandwich ELISA kits (Tanaka et al., unpublished).

Flow Cytometry (FCM)

Cells to be analyzed were Fc-blocked with 2 mg/ml normal human pooled IgG on ice for 15 minutes, and aliquots of these cells were subjected to staining using pre-determined optimum concentrations of fluorescent dye-conjugated mAbs for 30 minutes on ice. The cells were then washed using FACS buffer (PBS containing 2% FCS and 0.1% sodium azide), fixed in 1% paraformaldehyde (PFA) in FACS buffer and analyzed using a FACS Calibur. The data obtained were analyzed using the Cell Quest software (BD). For detection of HIV-1 infected cells, cells were fixed with 4% PFA-containing PBS for 5 min at room temperature followed by washing with 0.1% Saponin-containing FACS buffer. These cells were then Fc-blocked with 2 mg/ml normal human pooled IgG on ice for 15 min, and aliquots of these cells were stained with Alexa Fluor 488-conjugated anti-HIV-1 p24 mAb (clone 2C2) for 30 min on ice. The cells were then washed using FACS buffer and the frequency and the absolute number of p24+ cells determined by FCM using a cell counting kit (BD) according to the manufacturer's protocol.

Statistical analysis

Data were tested for significance using the Student's *t* test using the Prism software (GraphPad Software).

Additional material

Additional file 1: Dose response of the A120 mAb-mediated MIP-1α production in activated PBMCs. As described in the legend for Figure 7, activated PBMCs were incubated in the presence of graded concentrations of the A120 mAb or isotype control mAb for an additional day. Changes in the concentrations of MIP-1α in the culture supernatants were assayed by ELISA. Isotype control mAbs did not enhance MIP-1α production at 0.5~20 μg/ml in these culture conditions (data not shown). Representative data are from 3 independent experiments using PBMCs from a single donor.

Lists of abbreviations used

HIV: human immunodeficiency virus; PBMC: peripheral blood mononuclear cells; mAb: monoclonal antibody; X4: CXCR4-tropic; R5: CCR5-tropic; ECL: extra-cellular loop.

Acknowledgements

This work was supported by grants from the Ministry of Education, Culture, Sports, Science, and Technology and the Ministry of Health, Labor, and Welfare of Japan. We are grateful to Prof. Koyanagi of Kyoto University for providing stocks of HIV-1.

Author details

[1]Department of Immunology, Graduate School of Medicine, University of the Ryukyus, Okinawa, Japan. [2]Department of Pathology, Emory University School of Medicine, Atlanta, GA 30322, USA.

Authors' contributions

TA and RT performed research, analyzed data, and wrote the manuscript. AK, SM, and Takahashi contributed to experiments and analyzed data. AAA contributed to designing research and wrote the manuscript. YT designed and preformed research, wrote the manuscript and provided funding for this study. All authors read and approved the final manuscript.

Competing interests

The authors declare that they have no competing interests.

Received: 7 September 2011 Accepted: 22 October 2011
Published: 22 October 2011

References

1. Rodriguez-Frade JM, Mellado M, Martinez AC: **Chemokine receptor dimerization: two are better than one.** *Trends Immunol* 2001, **22**:612-617.
2. Thelen M, Munoz LM, Rodriguez-Frade JM, Mellado M: **Chemokine receptor oligomerization: functional considerations.** *Curr Opin Pharmacol* 2010, **10**:38-43.
3. Bleul CC, Farzan M, Choe H, Parolin C, Clark-Lewis I, Sodroski J, Springer TA: **The lymphocyte chemoattractant SDF-1 is a ligand for LESTR/fusin and blocks HIV-1 entry.** *Nature* 1996, **382**:829-833.
4. Feng Y, Broder CC, Kennedy PE, Berger EA: **HIV-1 entry cofactor: functional cDNA cloning of a seven-transmembrane, G protein-coupled receptor.** *Science* 1996, **272**:872-877.
5. Lusso P: **HIV and the chemokine system: 10 years later.** *EMBO J* 2006, **25**:447-456.
6. Wu B, Chien EY, Mol CD, Fenalti G, Liu W, Katritch V, Abagyan R, Brooun A, Wells P, Bi FC, *et al*: **Structures of the CXCR4 chemokine GPCR with small-molecule and cyclic peptide antagonists.** *Science* 2010, **330**:1066-1071.
7. Contento RL, Molon B, Boularan C, Pozzan T, Manes S, Marullo S, Viola A: **CXCR4-CCR5: a couple modulating T cell functions.** *Proc Natl Acad Sci USA* 2008, **105**:10101-10106.
8. Brelot A, Heveker N, Pleskoff O, Sol N, Alizon M: **Role of the first and third extracellular domains of CXCR-4 in human immunodeficiency virus coreceptor activity.** *J Virol* 1997, **71**:4744-4751.
9. Brelot A, Heveker N, Montes M, Alizon M: **Identification of residues of CXCR4 critical for human immunodeficiency virus coreceptor and chemokine receptor activities.** *J Biol Chem* 2000, **275**:23736-23744.
10. Chabot DJ, Zhang PF, Quinnan GV, Broder CC: **Mutagenesis of CXCR4 identifies important domains for human immunodeficiency virus type 1 X4 isolate envelope-mediated membrane fusion and virus entry and reveals cryptic coreceptor activity for R5 isolates.** *J Virol* 1999, **73**:6598-6609.
11. Doranz BJ, Orsini MJ, Turner JD, Hoffman TL, Berson JF, Hoxie JA, Peiper SC, Brass LF, Doms RW: **Identification of CXCR4 domains that addort coreceptor and chemokine receptor functions.** *J Virol* 1999, **73**:2752-2761.
12. Lu Z, Berson JF, Chen Y, Turner JD, Zhang T, Sharron M, Jenks MH, Wang Z, Kim J, Rucker J, *et al*: **Evolution of HIV-1 coreceptor usage through interactions with distinct CCR5 and CXCR4 domains.** *Proc Natl Acad Sci USA* 1997, **94**:6426-6431.
13. Kuritzkes DR: **HIV-1 entry inhibitors: an overview.** *Curr Opin HIV AIDS* 2009, **4**:82-87.
14. Rodriguez-Frade JM, del Real G, Serrano A, Hernanz-Falcon P, Soriano SF, Vila-Coro AJ, de Ana AM, Lucas P, Prieto I, Martinez AC, Mellado M: **Blocking HIV-1 infection via CCR5 and CXCR4 receptors by acting in trans on the CCR2 chemokine receptor.** *EMBO J* 2004, **23**:66-76.
15. Vila-Coro AJ, Mellado M, Martin de Ana A, Lucas P, del Real G, Martinez AC, Rodriguez-Frade JM: **HIV-1 infection through the CCR5 receptor is blocked by receptor dimerization.** *Proc Natl Acad Sci USA* 2000, **97**:3388-3393.
16. Tanaka R, Yoshida A, Murakami T, Baba E, Lichtenfeld J, Omori T, Kimura T, Tsurutani N, Fujii N, Wang ZX, *et al*: **Unique monoclonal antibody**

recognizing the third extracellular loop of CXCR4 induces lymphocyte agglutination and enhances human immunodeficiency virus type 1-mediated syncytium formation and productive infection. *J Virol* 2001, **75**:11534-11543.
17. Levy JA: **The search for the CD8+ cell anti-HIV factor (CAF).** *Trends Immunol* 2003, **24**:628-632.
18. Menten P, Wuyts A, Van Damme J: **Macrophage inflammatory protein-1.** *Cytokine Growth Factor Rev* 2002, **13**:455-481.
19. Mackay CR: **CCL3L1 dose and HIV-1 susceptibility.** *Trends Mol Med* 2005, **11**:203-206.
20. Nedellec R, Coetzer M, Lederman MM, Offord RE, Hartley O, Mosier DE: **Resistance to the CCR5 inhibitor 5P12-RANTES requires a difficult evolution from CCR5 to CXCR4 coreceptor use.** *PLoS One* 2011, **6**:e22020.
21. Tanaka Y, Zeng L, Shiraki H, Shida H, Tozawa H: **Identification of a neutralization epitope on the envelope gp46 antigen of human T cell leukemia virus type I and induction of neutralizing antibody by peptide immunization.** *J Immunol* 1991, **147**:354-360.
22. Inudoh M, Kato N, Tanaka Y: **New monoclonal antibodies against a recombinant second envelope protein of Hepatitis C virus.** *Microbiol Immunol* 1998, **42**:875-877.
23. Yoshida A, Tanaka R, Murakami T, Takahashi Y, Koyanagi Y, Nakamura M, Ito M, Yamamoto N, Tanaka Y: **Induction of protective immune responses against R5 human immunodeficiency virus type 1 (HIV-1) infection in hu-PBL-SCID mice by intrasplenic immunization with HIV-1-pulsed dendritic cells: possible involvement of a novel factor of human CD4(+) T-cell origin.** *J Virol* 2003, **77**:8719-8728.
24. Tanaka R, Takahashi Y, Kodama A, Saito M, Ansari AA, Tanaka Y: **Suppression of CCR5-tropic HIV type 1 infection by OX40 stimulation via enhanced production of beta-chemokines.** *AIDS Res Hum Retroviruses* 2010, **26**:1147-1154.
25. Matsuyama T, Hamamoto Y, Yoshida T, Kido Y, Kobayashi S, Kobayashi N, Yamamoto N: **Effect of culture supernatant of MT-2 cells on human immunodeficiency virus-producing cells, MOLT-4/HIVHTLV-IIIB cells.** *Jpn J Cancer Res* 1988, **79**:156-159.
26. Yoshida M, Miyoshi I, Hinuma Y: **A retrovirus from human leukemia cell lines: its isolation, characterization, and implication in human adult T-cell leukemia (ATL).** *Princess Takamatsu Symp* 1982, **12**:285-294.

doi:10.1186/1742-4690-8-84
Cite this article as: Adachi *et al.*: Identification of an unique CXCR4 epitope whose ligation inhibits infection by both CXCR4 and CCR5 tropic human immunodeficiency type-I viruses. *Retrovirology* 2011 **8**:84.

The American Journal of Pathology, Vol. 180, No. 3, March 2012

DOI: 10.1016/j.ajpath.2011.11.012

Cell Injury, Repair, Aging, and Apoptosis

Decreased Proteasomal Activity Causes Age-Related Phenotypes and Promotes the Development of Metabolic Abnormalities

Utano Tomaru,* Satomi Takahashi,* Akihiro Ishizu,† Yukiko Miyatake,* Aya Gohda,* Sayuri Suzuki,* Ayako Ono,* Jiro Ohara,* Tomohisa Baba,‡ Shigeo Murata,§ Keiji Tanaka,¶ and Masanori Kasahara*

From the Department of Pathology, Hokkaido University Graduate School of Medicine, Sapporo; the Faculty of Health Sciences,† Hokkaido University, Sapporo; the Division of Molecular Bioregulation,‡ Cancer Research Institute, Kanazawa University, Kanazawa; the Laboratory of Protein Metabolism,§ Graduate School of Pharmaceutical Science, The University of Tokyo, Tokyo; and the Laboratory of Protein Metabolism,¶ Tokyo Metropolitan Institute of Medical Science, Tokyo, Japan*

The proteasome is a multicatalytic enzyme complex responsible for the degradation of both normal and damaged proteins. An age-related decline in proteasomal activity has been implicated in various age-related pathologies. The relevance of decreased proteasomal activity to aging and age-related diseases remains unclear, however, because suitable animal models are not available. In the present study, we established a transgenic (Tg) mouse model with decreased proteasomal chymotrypsin-like activity. Tg mice exhibited a shortened life span and developed age-related phenotypes. In Tg mice, polyubiquitinated and oxidized proteins accumulated, and the expression levels of cellular proteins such as Bcl-xL and RNase L were altered. When Tg mice were fed a high-fat diet, they developed more pronounced obesity and hepatic steatosis than did wild-type mice. Consistent with its role in lipid droplet formation, the expression of adipose differentiation-related protein (ADRP) was elevated in the livers of Tg mice. Of note, obesity and hepatic steatosis induced by a high-fat diet were more pronounced in aged than in young wild-type mice, and aged wild-type mice had elevated levels of ADRP, suggesting that the metabolic abnormalities present in Tg mice mimic those in aged mice. Our results provide the first *in vivo* evidence that decreased proteasomal chymotrypsin-like activity affects longevity and aggravates age-related metabolic disorders, such as obesity and hepatic steatosis. *(Am J Pathol 2012, 180:963–972; DOI: 10.1016/j.ajpath.2011.11.012)*

Protein degradation is a major intracellular function, responsible not only for cellular housekeeping but also for regulation of important cellular functions. Two major proteolytic systems are responsible for most intracellular protein turnover: the lysosomal system and the ubiquitin (Ub) proteasome system.[1] The latter contributes to the maintenance of cellular homeostasis and protein quality control, and functions as a regulator of many essential cellular processes, including proliferation, cell cycling, gene transcription, apoptosis, antioxidant responses, and immune reactions.[2,3] Proteasomes are multisubunit complexes made up of a core particle, known as the 20S proteasome, and additional subunits comprising the 19S complex. Proteolysis is conducted by three β subunits, β1, β2, and β5, which have caspase-like, trypsin-like, and chymotrypsin-like activities, respectively.[4] It has been assumed that the relative importance of the three proteolytic activities varies across substrates and depends on the proteins being degraded.[5] However, little is known about the importance of each proteasomal activity *in vivo*.

Recently, the proteasome has emerged as an attractive target for cancer therapy, because proteasome inhibition has produced encouraging antitumor activity in preclinical studies and clinical trials. Bortezomib (originally codenamed PS-341), the first proteasome inhibitor tested in clinical trials, has been used for treating multiple myeloma patients.[6] This drug has also been shown to be effective with manageable toxicity for mantle cell and other lymphomas, leukemias, and solid malignancies, in-

Supported in part by grants-in-aid for scientific research from the Ministry of Education, Culture, Sports, Science and Technology of Japan (U.T.).

Accepted for publication November 4, 2011.

Supplemental material for this article can be found at *http://ajp.amjpathol.org* or at doi: 10.1016/j.ajpath.2011.11.012.

Address reprint requests to Utano Tomaru, M.D., Ph.D., Kita-15, Nishi-7, Kita-ku, Sapporo 060-8638, Japan. E-mail: tomaruu@med.hokudai.ac.jp.

cluding non-small cell lung carcinoma.[6] Although different factors regulate apoptosis in individual carcinoma cell models, it is plausible that bortezomib promotes apoptosis by shifting the balance from antiapoptotic signals toward proapoptotic signals through modulation of the translocation of nuclear factor-κB (NF-κB).[7]

Physiologically, proteasomal activity decreases with age.[8–11] Because the proteasome plays an essential role in cellular processes, an age-associated decline in proteasome function is assumed to contribute to the development of age-related pathology and to the aging process itself.[10] Indeed, recent evidence indicates that mouse hepatocytes with impaired assembly of 20S proteasomes undergo premature senescence.[12] Furthermore, reduced 26S proteasome assembly in *Drosophila* was shown to shorten life span and enhance the development of neurodegenerative phenotypes.[11] Nonetheless, there is no direct evidence linking decreased 20S proteasomal activity and age-related pathology in mammals, because in mice deficiency in catalytic subunits β1, β2, or β5 is lethal, and no other suitable animal models are available.

In the present study, we generated transgenic (Tg) mice with decreased proteasomal chymotrypsin-like activity by introducing mouse β5t as a transgene. β5t is a recently discovered β5-like subunit of the 20S proteasome expressed exclusively in the thymus.[13] In the thymic cortex, β5t is incorporated into 20S proteasomes in place of β5 or β5i and forms a specialized type of proteasomes, known as thymoproteasomes, that seem to be important for positive selection of T cells.[13–15] Because β5t has only weak chymotrypsin-like activity and seems to be preferentially incorporated into 20S proteasomes over β5 or β5i,[16] we reasoned that forced expression of this subunit *in vivo* would generate an animal model with decreased proteasomal chymotrypsin-like activity. We show here that the reduction of proteasomal chymotrypsin-like activity *in vivo* results in a shortened life span and the development of age-related phenotypes. We also show that mice with decreased proteasomal chymotrypsin-like activity develop more profound obesity and hepatic steatosis than wild-type (WT) mice when challenged with a high-fat diet (HFD).

Materials and Methods

Generation of Tg Mice and Animal Experiments

Mouse β5t cDNA was ligated to the CAGGS vector,[17] which allows for ubiquitous expression of a transgene under the control of the cytomegalovirus immediate-early enhancer and the chicken-actin promoter/enhancer. The expression construct was injected into C57BL/6 fertilized ova; integration of the β5t transgene was detected in three of the pups born from the DNA-injected ova. The transgene was transmitted into the offspring in two independently derived transgenic lines. Both transgenic lines showed similar phenotypes, with low weight and a short life span, compared with WT littermates. Both Tg and WT mice were housed on a 12-hour light-dark cycle in climate-controlled, pathogen-free barrier facilities. For feeding experiments, 6-week-old Tg and WT male mice were fed a HFD or a normal control diet (CD) (HFD-60 or AIN-93G; Oriental Yeast, Tokyo, Japan) and water *ad libitum* for 16 weeks. For aged mice, we used 76-week-old WT mice; they were fed HFD or CD for 16 weeks. All animal experiments were conducted according to the Guidelines for the Care and Use of Laboratory Animals at Hokkaido University Graduate School of Medicine.

Cell Isolation and Cell Culture

Primary fibroblastic cells (FCs) and hepatocytes were isolated from Tg and WT male mice using collagenase digestion. FCs were grown in Dulbecco's modified Eagle's medium supplemented with 20% fetal bovine serum, 100 U/mL penicillin, and 100 U/mL streptomycin in an atmosphere of 5% CO_2 and 95% O_2 at 37°C. FCs were assayed for proteasomal activity during passages 3 to 4; primary hepatocytes were assayed immediately after isolation. FCs from WT mice were treated with 5 to 50 nmol/L of bortezomib (Janssen Pharmaceuticals, Tokyo, Japan) for 20 hours and subjected to Western blot analysis. Hepatocytes from WT mice were incubated in oleic acid-containing medium (600 μmol/L) with or without 100 nmol/L bortezomib for 48 hours and then were subjected to staining with Oil Red O (Sigma-Aldrich, St. Louis, MO) and Western blot analysis.

Histological Analysis

Formalin-fixed tissue sections were stained with H&E. The thickness of the dermal adipose and muscle layers was quantified by random measurements of the length of individual skin samples. To estimate lipid accumulation, frozen liver sections or isolated primary hepatocytes were stained with Oil Red O solution. For immunohistochemical detection of Ub, tissue slides were processed for antigen retrieval by a standard microwave heating technique, and incubated with anti-Ub antibody (Ab) (DakoCytomation Japan, Tokyo, Japan), followed by detection with streptavidin-biotin-horseradish peroxidase (DakoCytomation Japan). To detect aggresomes, FCs were cultured in chamber slides, and slides were stained according to the manufacturer's instructions (ProteoStat aggresome detection kit; Enzo Life Sciences, Farmingdale, NY; Lausen, Switzerland). For immunofluorescence staining for adipose differentiation-related protein (ADRP), hepatocytes on chamber slides were washed twice in PBS, fixed with 4% paraformaldehyde for 30 minutes, and permeabilized with 0.1% Triton-X surfactant in PBS for 5 minutes. After a washing, the slides were incubated in PBS with 10% goat serum for 1 hour at room temperature, followed by overnight incubation with anti-ADRP Ab (Abcam Japan, Tokyo, Japan) at 4°C. Sections were stained with BODIPY 493/503 (Invitrogen, Tokyo, Japan) to detect intracellular lipid, and labeled with Alexa Fluor 594-conjugated goat anti-chicken IgG (Invitrogen) and Hoechst 33342 dye (Enzo Life Sciences) for nuclear staining.

Immunoprecipitation and Western Blot Analysis

Tissues were lysed in a buffer containing 150 mmol/L NaCl, 20 mmol/L Tris-HCl (pH 7.5), 0.2% NP-40 detergent, and 1 mmol/L dithiothreitol, and centrifuged at 15,000 × *g* for 10 minutes. The supernatants (10 μg aliquot of total proteins) were subjected to SDS-PAGE and blotted onto nitrocellulose membranes. The blots were probed with Abs, and reacted with horseradish peroxidase-conjugated anti-rabbit IgG (Jackson ImmunoResearch, West Grove, PA) for immunodetection. The immune complexes were visualized by enhanced chemiluminescence (Amersham; GE Healthcare, Piscataway, NJ) and analyzed by Image Gauge software version 2.1 (Fujifilm, Tokyo, Japan). For immunoprecipitation, tissue lysates (100 μg of protein) were incubated in a total volume of 150 μL of 25 mmol/L Tris-HCl buffer (pH 7.5) containing 1 mmol/L dithiothreitol at 4°C for 2 hours with Abs bound to protein A Sepharose (Amersham). The beads were washed and boiled in SDS sample buffer. After centrifugation, supernatants were used for Western blot analysis. Each lane was loaded with 15% of the total amount of proteasomes precipitated with Abs. The Abs for β5, β5i, β5t, and α6 were as described previously.[13] The Abs for RNase L were purchased from Santa Cruz Biotechnology (Santa Cruz, CA); the Abs for Bcl-xL were purchased from Sigma-Aldrich. The Abs for cell death-inducing DNA fragmentation factor-45-like effector protein (CIDE) A, CIDE B, fat-specific protein 27 (Fsp 27), and perilipin A were purchased from Abcam Japan. The Ab for Ub was purchased from Enzo Life Sciences. These antibodies were used according to the manufacturers' recommendations. All information, including the dilution and organism, may be provided via data sheets form the companies.

Measurement of Proteasomal Activity

FCs and hepatocytes were harvested into 96-well plates at 10,000 cells per well and were analyzed using proteasome activity assay kits (Proteasome-Glo cell-based assay; Promega, Madison, WI), according to the manufacturer's instructions. Briefly, cells were incubated with specific luminogenic proteasome substrates (Suc-LLVY-aminoluciferin for chymotrypsin-like activity, Z-LRR-aminoluciferin for trypsin-like activity, and Z-nLPnLD-aminoluciferin for caspase-like activity), and substrate luminescence was measured by a luminometer. The number of viable cells in each well was measured by ATP measurement methods using luciferase reactions (CellTiter-Glo luminescent cell viability assay; Promega). All data were corrected by the number of viable cells and expressed as a substrate luminescence/ATP luminescence ratio. All measurements were made in triplicate.

Cellular Senescence Assay

To detect senescence-associated β-galactosidase, FCs in subconfluent cultures were stained using a cellular senescence assay kit (Cell Biolabs, San Diego, CA). Briefly, cells were washed with PBS, fixed for 5 minutes with fixing solution, and washed again with PBS. Cells were incubated overnight at 37°C in a CO_2-free atmosphere with senescence-associated β-galactosidase staining solution. Positive cells were scored under light microscopy.

Laboratory Data and Measurement of Triglycerides and Cholesterol

Tail blood was collected and centrifuged to obtain clear sera. Blood total protein, albumin, aspartate transaminase, lactate dehydrogenase, and cholesterol levels were measured at the Kishimoto Clinical Laboratory (Sapporo, Japan). Serum leptin and insulin levels were determined via enzyme-linked immunosorbent assay, according to the manufacturer's instructions, at the Morinaga Institute of Biological Science (Tokyo, Japan). For glucose tolerance tests, mice fed the CD or a HFD for 12 weeks were fasted for 12 hours with full access to water. Fasted mice were administered D-glucose solution intraperitoneally at 1 g/kg body weight. At 0, 30, 60, or 120 minutes after administration, blood glucose levels were measured using a measuring device (OneTouch UltraVue; Johnson & Johnson, Tokyo, Japan). Triglycerides and cholesterol in the liver tissue were measured at Skylight Biotech (Tokyo, Japan).

Protein Assays

Muscles were lysed in a buffer containing 150 mmol/L NaCl, 20 mmol/L Tris-HCl (pH 7.5), 0.2% NP-40, and 1

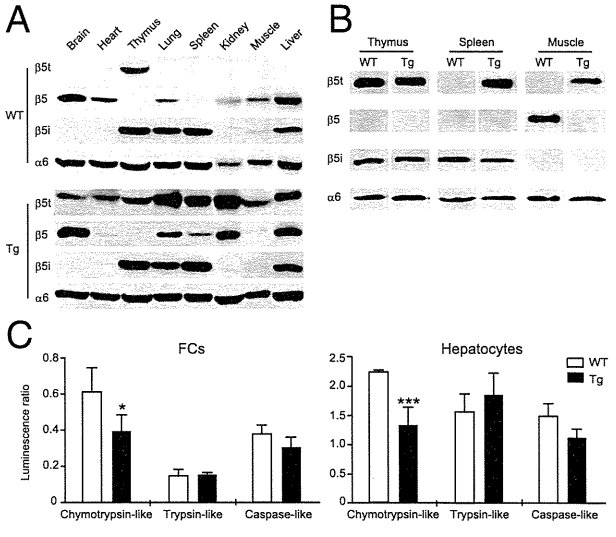

Figure 1. β5t is ubiquitously expressed and incorporated into 20S proteasomes in Tg mice. **A:** Expression of β5t in WT and Tg mice. Tissue extracts were immunoblotted with β5t, β5, β5i, and α6 Abs. Tissue distribution of β5 and β5i was similar in WT and Tg mice. **B:** Incorporation of β5t into 20S proteasomes in Tg mice. Extracts from thymus, spleen, and skeletal muscle were immunoprecipitated with Ab for α6, followed by immunoblotting with the same four Abs. β5t was incorporated into 20S proteasomes in the tissues of Tg mice. β5-containing 20S proteasomes virtually disappeared from the muscle of Tg mice. In the spleen of Tg mice, β5i-containing 20S proteasomes were detected along with β5t-containing 20S proteasomes. **C:** Proteasomal activities in Tg mice. FCs and hepatocytes isolated from WT or Tg mice were subjected to cell-based luminescence assays using specific luminogenic proteasome substrates: Suc-LLVY-aminoluciferin for chymotrypsin-like activity, Z-LRR-aminoluciferin for trypsin-like activity, and Z-nLPnLD-aminoluciferin for caspase-like activity. The number of viable cells was measured by ATP assays using the luciferase reaction. Chymotrypsin-like activity was significantly decreased in FCs and hepatocytes from Tg mice. Data are expressed as the substrate luminescence/ATP luminescence ratio (mean ± SD). $n = 4$ mice per group. $^{*}P < 0.05$, $^{***}P < 0.001$ versus WT (Student's *t*-test).

mmol/L dithiothreitol, and centrifuged at 15,000 × *g* for 10 minutes. The levels of polyubiquitinated proteins were quantified by enzyme-linked immunosorbent assay according to the manufacturer's instructions (CycLex, Nagano, Japan). Levels of oxidized proteins were determined by sensitive procedures based on the reactivity of protein carbonyl with 2,4-dinitrophenylhydrazine,[18,19] using an ELISA kit according to the manufacturer's instructions (BioCell, Auckland, New Zealand). Protein expression profiles were compared in muscles of WT and Tg mice with a Panorama antibody microarray XPRESS Profiler725 kit (Sigma-Aldrich), according to the manufacturer's instructions. Briefly, extracts from muscles of WT and Tg (1 mg/mL) were labeled with Cy3 and Cy5 dyes, respectively, and the samples were applied simultaneously on the array. The expression profile of each sample (Cy3 and Cy5) was recorded individually and compared. The microarray slides were scanned on a GenePix 4000B scanner (Molecular Devices Japan, Tokyo, Japan). Data were normalized, and the ratio of Tg to WT mice was computed for each spot, to estimate the relative fold excess.

Image Analyses

The thickness of the dermal adipose and muscle layers, the amount of lipid accumulation in liver tissues and hepatocytes, and Western blotting data were subjected to image analysis using ImageJ software version 1.43u (NIH, Bethesda, MD).

Statistical Analyses

We performed statistical analyses for two unmatched groups with the unpaired, two-tailed Student's *t*-test. For the analysis of three or more unmatched groups, one-way analysis of variance with multiple comparisons or post hoc testing was performed. *P* values of <0.05 were considered significant.

Results

Decreased Body Weight and a Shortened Life Span in Tg Mice

In Tg mice, β5t was expressed in all of the tissues tested and was incorporated into 20S proteasomes, whereas in WT mice β5t was expressed only in the thymus (Figure 1, A and B). As expected, proteasomes in Tg mice showed decreased chymotrypsin-like activity, compared with those in WT mice (Figure 1C).

Tg mice were smaller in size and weighed significantly less than WT mice (Figure 2A). Furthermore, the survival rate was markedly reduced; more than half of the Tg mice died by 40 weeks (Figure 2B). Tg and WT mice showed similar food intake (Figure 2C), and their blood total pro-

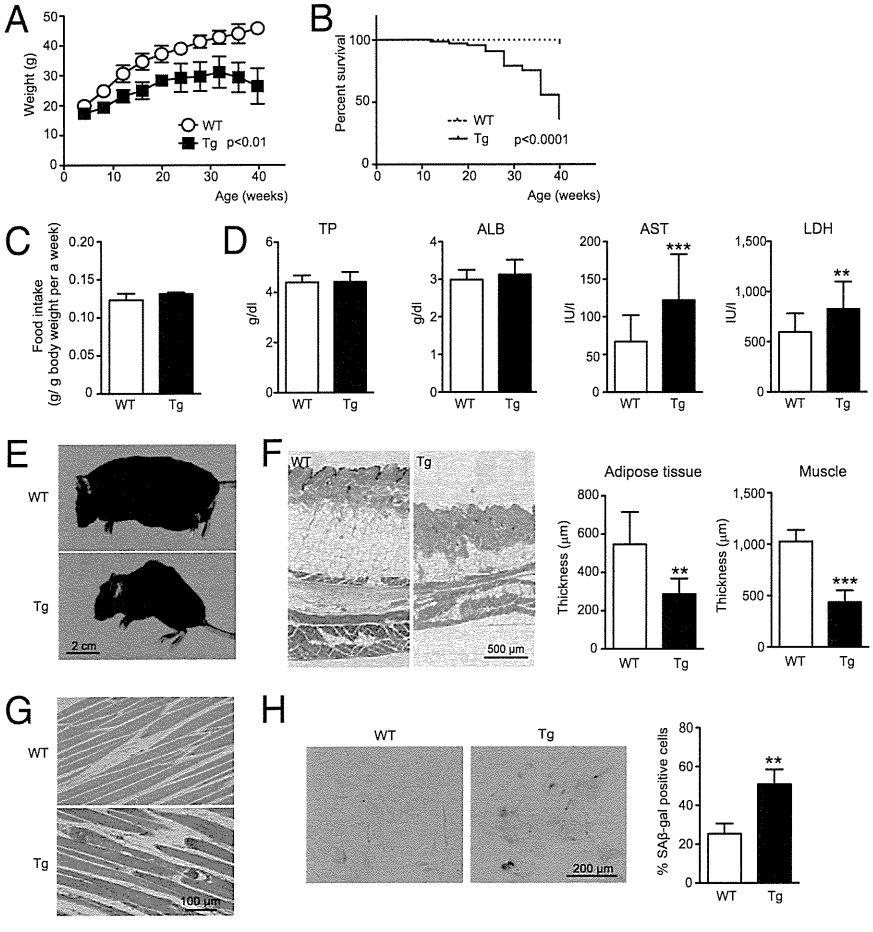

Figure 2. Decreased body weight and shortened life span in Tg mice. **A:** Body weight of male WT and Tg mice. $n = 6$ to 10 mice per data point. **B:** Kaplan-Meier survival analysis of WT ($n = 70$) and Tg ($n = 75$) cohort mice. **C:** Food intake was measured for 4 weeks in 16-week-old WT and Tg mice. $n = 4$ mice per group. **D:** Plasma concentrations of total protein (TP), albumin (ALB), aspartate transaminase (AST), and lactate dehydrogenase (LDH) in WT and Tg mice. All mice were 4 to 24 weeks old. $n = 24$ mice per group. **E:** Representative photographs of 24-week-old WT and Tg mice. Tg mice were smaller and appeared weak, compared with WT mice, and frequently exhibited lordokyphosis. Scale bar = 2 cm. **F:** Subcutaneous adipose tissue and muscle mass in Tg mice (24 weeks of age) were decreased. The thickness was measured as described under *Materials and Methods*. All mice were 24 weeks old. $n = 6$ mice per group. Scale bar = 500 μm. **G:** Representative histological sections of skeletal muscle in WT and Tg mice. Atrophy and degeneration of muscle fibers appeared frequently in Tg mice older than 24 weeks of age. Scale bar = 100 μm. **H:** Cellular senescence in FCs from Tg mice. FCs from WT and Tg mice were stained with senescence-associated β-galactosidase solution. Positive cells were scored under light microscopy. $n = 3$ mice per group. Scale bar = 200 μm. Data are expressed as means ± SD. $^{**}P < 0.01$, $^{***}P < 0.001$ versus WT (Student's *t*-test).

tein and albumin levels were also similar (Figure 2D). Aspartate transaminase and lactate dehydrogenase levels were significantly increased in Tg mice (Figure 2D). Tg mice younger than 12 weeks of age displayed no apparent histological abnormality (see Supplemental Figure S1 at *http://ajp.amjpathol.org*). After 24 weeks of age, Tg mice gradually became weak, and died without any gross pathological changes such as cancer and cardiovascular diseases (data not shown). They frequently exhibited lordokyphosis (curvature of the spinal column) and a loss of subcutaneous adipose tissue and skeletal muscle mass (Figure 2, E and F). Microscopically, degeneration of skeletal muscle fibers was observed (Figure 2G). There were no phenotypic differences between male and female Tg mice (data not shown). Lordokyphosis and the loss of subcutaneous fat and skeletal muscle mass are prominent features of aging. In addition, primary FCs from Tg mice showed elevated levels of senescence-associated β-galactosidase, compared with those from age-matched WT mice (Figure 2H). Thus, these results suggest that decreased chymotrypsin-like activity induces cellular senescence and leads to a shortened life span and age-related phenotypes.

Accumulation of Polyubiquitinated and Oxidized Proteins in Tg Mice

Proteasomes are responsible for the degradation of normal cellular proteins, as well as of abnormal proteins such as misfolded and oxidized proteins. We therefore investigated whether protein degradation by proteasomes is impaired in Tg mice. First, we investigated whether polyubiquitinated proteins are accumulated in the tissue lysates from muscles of Tg mice. Polyubiquitinated proteins were significantly increased in Tg mice (Figure 3A). Immunohistochemical analysis showed accumulation of Ub-conjugated substrates in both the nucleus and cytoplasm (Figure 3B). In addition, aggresomes were observed in FCs from Tg mice (see Supplemental Figure S2 at *http://ajp.amjpathol.org*). Next, using a protein array, we compared the expression of 725 proteins regulating cellular functions including apoptosis, cell cycle, signal transduction, and stress responses between Tg and WT mice. Expression of several cellular proteins was significantly altered in Tg mice (see Supplemental Table S1 at *http://ajp.amjpathol.org*). Notably, two cellular proteins regulating cellular senescence and survival showed altered expression: RNase L was increased more than twofold, and Bcl-xL was reduced more than twofold in Tg mice. These findings were confirmed by Western blot analysis (Figure 3C).

To examine whether the accumulated RNase L proteins in Tg mice are polyubiquitinated, immunoprecipitates with anti-RNase L Ab were analyzed by Western blotting using anti-Ub Ab (Figure 3D). RNase L proteins in Tg mice were polyubiquitinated, suggesting that the accumulation of RNase L proteins is due to decreased protein degradation resulting from decreased proteasomal activity. We tested the influence of proteasome inhibition on the level of RNase L proteins by *in vitro* experiments using the proteasome inhibitor bortezomib.

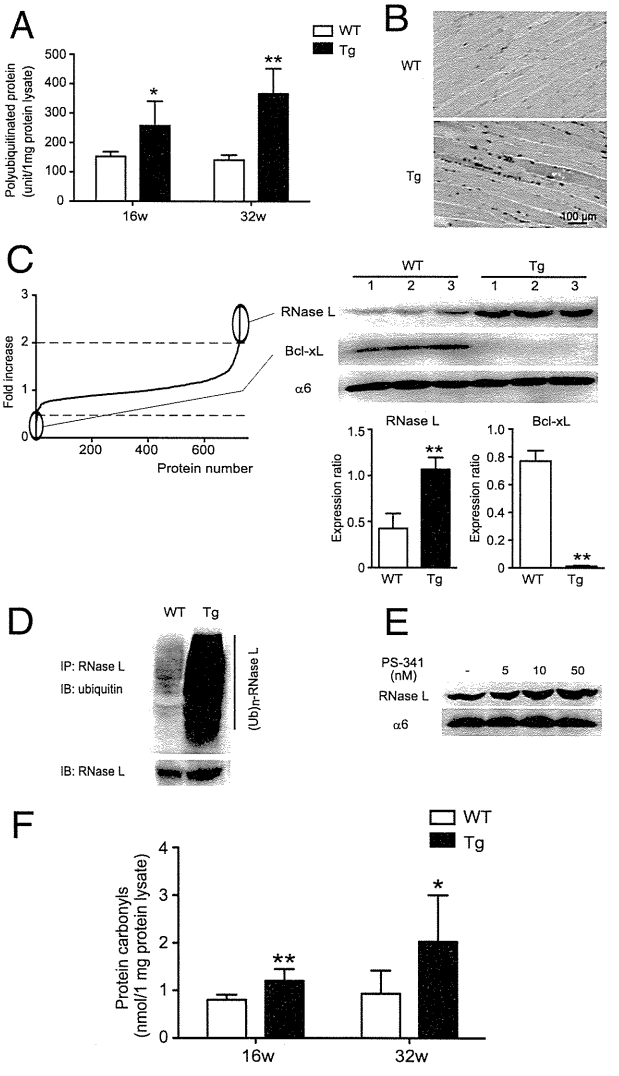

Figure 3. Accumulation of polyubiquitinated and oxidized proteins in Tg mice. **A:** Polyubiquitinated proteins in the muscles of WT and Tg mice at 16 and 32 weeks. $n = 4$ mice per group. **B:** Immunohistochemical staining for Ub in the muscles of 24-week-old WT and Tg mice. Staining patterns are representative of four WT and four Tg mice. Scale bar = 100 μm. **C:** Altered expression of cellular proteins in Tg mice. Expression levels of 725 proteins extracted from skeletal muscles were compared between 24-week-old WT and Tg mice. Proteins whose expression levels differed more than twofold between WT and Tg mice are encircled. A comprehensive list of proteins with altered expression is given in Supplemental Table S1 (available at *http://ajp.amjpathol.org*). Altered expression of RNase L and Bcl-xL was validated by Western blot analysis. Lanes 1, 2, and 3 represent individual mice. The proteasome subunit α6 was used as an internal control. The expression ratio of RNase L and Bcl-xL to α6 (**right upper panel**) was determined by image analysis of the Western blotting data (**right lower panel**). **D:** Polyubiquitinated RNase L is accumulated in Tg mice. Muscle tissue extracts from 24-week-old WT and Tg mice were immunoprecipitated (IP) with anti-RNase L Ab, followed by immunoblotting (IB) with anti-Ub Ab. PolyUb-conjugated RNase L proteins typically appear as broad smears. **E:** RNase L accumulates in FCs treated with bortezomib (PS-341). FCs from WT mice were incubated in culture medium with 0, 5, 10, or 50 nmol/L of bortezomib for 18 hours. After incubation, samples were subjected to Western blot analysis. **F:** Protein carbonyl concentrations in the muscles of WT and Tg mice at 16 and 32 weeks. $n = 6$ mice per group. Data are expressed as means ± SD. $^*P < 0.05$, $^{**}P < 0.01$ versus WT (Student's *t*-test).

The degradation of RNase L was inhibited by bortezomib in a concentration-dependent manner (Figure 3E). Because proteasomal activity decreases with age,[8–11] we compared expression of Bcl-xL and RNase L between young (16 weeks old) and aged (92 weeks old) WT mice.

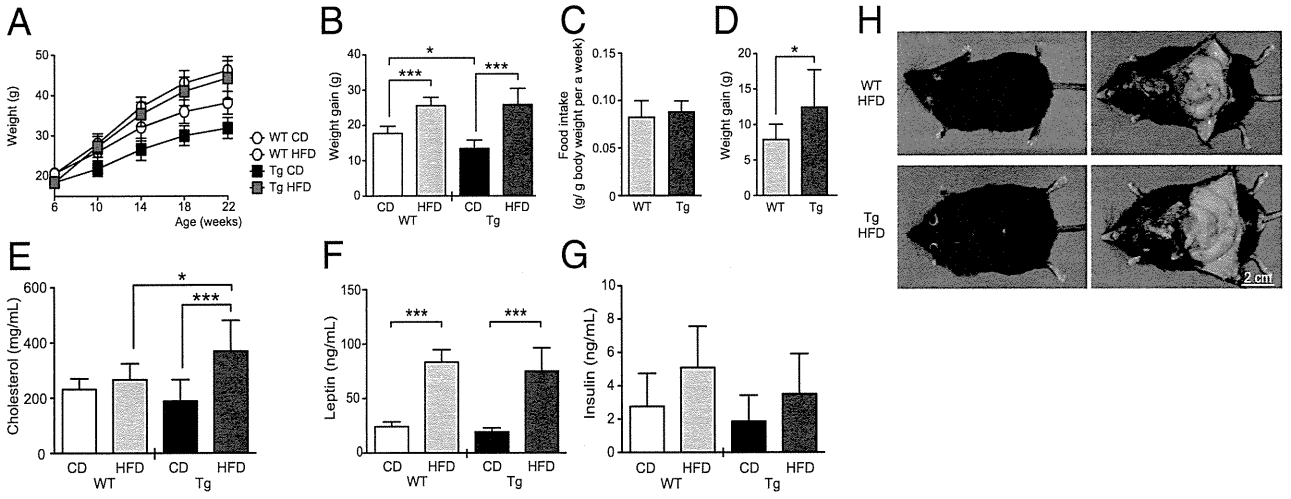

Figure 4. Obesity in HFD-fed Tg mice. **A:** Body weight of CD- or HFD-fed WT and Tg mice. $n = 10$ mice per data point. **B:** Weight gain in CD- or HFD-fed WT and Tg mice between the starting point (6 weeks old) and the endpoint (22 weeks old). $n = 10$ mice per group. **C:** Food intake in HFD-fed WT and Tg mice was measured for 4 weeks in 16-week-old WT and Tg mice. $n = 5$ mice per group. **D:** Weight gain after HFD feeding, calculated as the difference in body weight between CD-fed and HFD-fed mice. **E:** Total blood cholesterol concentrations in CD- or HFD-fed WT and Tg mice. **F** and **G:** Serum leptin (**F**) and insulin (**G**) concentrations in WT and Tg mice fed a CD or HFD. Data were collected at the endpoint (22 weeks old). $n = 10$ mice per group. **H:** Representative photographs of HFD-fed WT and Tg mice. HFD-fed Tg mice were visibly more obese, and the deposition of subcutaneous and visceral fat was more pronounced, compared with HFD-fed WT mice. Scale bar = 2 cm. Data are expressed as means ± SD. $^{*}P < 0.05$, $^{***}P < 0.001$ (one-way analysis of variance with multiple comparisons or post hoc testing).

Although expression of Bcl-xL was not significantly altered in aged WT mice, expression of RNase L was increased in aged WT mice, compared with young WT mice (see Supplemental Figure S3 at *http://ajp.amjpathol.org*).

We also measured protein carbonyl concentrations in the muscle as indices of oxidized proteins. In Tg mice, carbonylated proteins were increased (Figure 3F), indicating accumulation of oxidatively damaged proteins.

Pronounced Obesity and Fat Accumulation in HFD-Fed Tg Mice

Because proteasomal activity decreases with age, we hypothesized that a decline in proteasomal chymotrypsin-like activity *in vivo* might be involved in the development of age-related metabolic disorders. To test this hypothesis, we fed Tg mice a HFD and analyzed phenotypic alterations. Dietary fat is an important environmental factor promoting obesity, which in turn is critically involved in the development of many metabolic disorders. Administration of the HFD yielded more weight gain, compared with a CD, in both Tg and WT mice (Figure 4, A and B). There was no difference in food intake between WT and Tg mice fed a HFD (Figure 4C). Of note, when Tg and WT mice were fed a HFD, the Tg mice gained more weight than the WT mice (Figure 4D), and total blood cholesterol levels increased more prominently in Tg than in WT mice (Figure 4E). Serum leptin was also elevated in both Tg and WT mice fed a HFD; however, the increase was not significantly different between Tg and WT mice (Figure 4F). There was no significant increase in the levels of serum insulin (Figure 4G). Fasting serum glucose levels were significantly increased in both WT and Tg mice fed a HFD, compared with CD ($P < 0.05$); however, there was no significant difference in glucose tolerance between WT and Tg mice fed a HFD or between WT and Tg mice fed the CD (see Supplemental Figure S4 at *http://ajp.amjpathol.org*). Consistent with more weight gain, HFD feeding induced more prominent subcutaneous and visceral fat deposition in Tg than in WT mice (Figure 4H).

Microscopically, marked hepatic steatosis was observed in both Tg and WT mice; however, the pattern of steatosis was different. Tg mice developed macrovesicular steatosis, whereas lipid droplets in WT mice were predominantly microvesicular (Figure 5A). Tg mice accumulated more lipids than WT mice, as measured by digital image analysis of Oil Red O-stained liver sections (Figure 5B). Although there was no statistical difference, triglyceride and cholesterol levels in the liver of HFD-fed Tg mice were increased, compared with HFD-fed WT mice (see Supplemental Figure S5 at *http://ajp.amjpathol.org*). Because lipid-droplet-associated proteins, such as perilipin, ADRP, and CIDE family proteins (CIDE A, CIDE B, and Fsp27), are known to associate with intracellular lipid droplets and to regulate their formation and metabolism,[20,21] we examined their expression in the liver of Tg and WT mice. Among the proteins tested, expression of ADRP was significantly elevated in Tg mice (Figure 5C).

To examine whether decreased proteasomal activity promotes lipid accumulation, we performed *in vitro* experiments using primary hepatocytes. When hepatocytes isolated from WT mice were incubated in oleic acid-containing medium (600 μmol/L), Oil Red O-stained lipid droplets were observed in hepatocytes (Figure 6A). When the cells were treated with bortezomib, the amount of lipid droplets was significantly increased and the size of lipid droplets in the hepatocytes was enlarged (Figure 6, A and B). Expression of ADRP was elevated when the cells were incubated with oleic acid and bortezomib (Figure 6C), with ADRP distributed around lipid droplets in

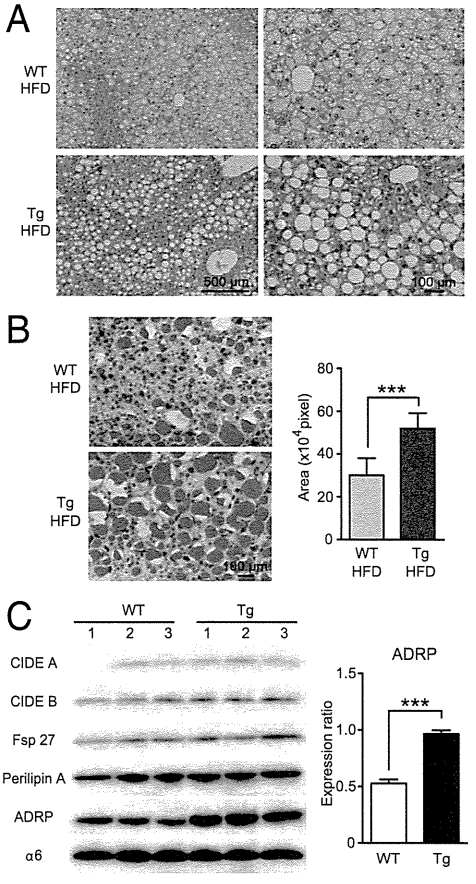

Figure 5. Steatosis and fat accumulation in HFD-fed Tg mice. **A:** H&E staining of liver sections from HFD-fed WT and Tg mice. Scale bars: 500 μm (**left**); 100 μm (**right**). **B:** Oil Red O staining of liver sections from HFD-fed WT and Tg mice. The amount of accumulated lipid in the liver of HFD-fed WT and Tg mice was measured by digital image analysis. $n = 10$ mice per group. **C:** Expression of lipid-droplet-associated proteins in Tg mice. Extracts from livers of 24-week-old WT and Tg mice were immunoblotted with six different Abs. Lanes 1, 2, and 3 represent individual mice. $n = 3$ mice per group. ADRP, adipose differentiation-related protein; CIDE A and B, cell death-inducing DNA fragmentation factor-45-like effector protein A and B; Fsp 27, fat-specific protein 27. The expression ratio of ADRP to α6 was determined by image analysis of the Western blotting data. Data are expressed as means ± SD. $^{***}P < 0.001$ (Student's *t*-test).

hepatocytes (see Supplemental Figure S6 at *http://ajp.amjpathol.org*). These results indicate that decreased proteasomal activity promotes lipid accumulation, suggesting a possible mechanistic explanation for the obesity and hepatic steatosis observed in Tg mice.

Pronounced Steatosis and Fat Accumulation in HFD-Fed Aged WT Mice

Although the underlying molecular mechanism is poorly understood, proteasomal activities are known to decrease with age.[8–11] We confirmed that hepatocytes from aged WT mice indeed had decreased proteasomal chymotrypsin-like activity, compared with those from young WT mice (Figure 7A). Tg mice showed significantly decreased chymotrypsin-like activity in comparison with age-matched WT mice; after 60 weeks of age, the chymotrypsin-like activities in WT mice were similar to those in Tg mice. To examine whether aged WT mice show metabolic abnormalities similar to those observed in Tg mice, 76-week-old WT mice were challenged with a HFD or CD. HFD feeding induced a significant increase in body weight and blood cholesterol levels, compared with CD feeding (Figure 7, B–D). Notably, a significant increase in blood cholesterol levels was observed in HFD-fed aged WT mice, but no significant increase was observed in HFD-fed young WT mice (Figures 4E and 7D). When young and aged mice were fed a HFD, aged mice gained more weight than young mice (Figure 7E). Strikingly, like the Tg mice (Figure 5, A and B), the HFD-fed aged mice developed macrovesicular hepatic steatosis (Figure 7F) and accumulated more lipids, compared with HFD-fed young mice (Figure 7G). In addition, ADRP expression was increased in aged mice (Figure 7H). Thus, Tg and aged WT mice exhibited similar metabolic abnormalities, and they both developed more pronounced obesity and hepatic steatosis than young WT mice when challenged with a HFD.

Discussion

An age-related decrease in proteasomal activity has been assumed to be involved in the aging process and the development of age-related pathology.[8–10] To date, however, evidence supporting this assumption has been limited. In the present study, we generated for the first time an animal model in which proteasomal chymotrypsin-like activity is reduced. Mice with diminished chymotrypsin-like activity accumulated ubiquitinated as well as oxidized proteins (Figure 3), and their life span was shortened, with evidence of cellular senescence (Figure 2). They exhibited lordokyphosis and a loss of subcutaneous adipose tissue and skeletal muscle mass (Figure 2), both prominent features of normal aging. Importantly, these mice showed metabolic abnormalities typically seen in aged mice; they were susceptible to HFD-induced obesity and hepatic steatosis, and had elevated levels of

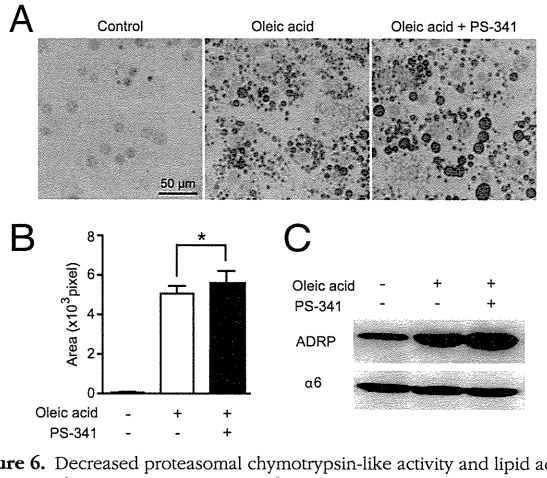

Figure 6. Decreased proteasomal chymotrypsin-like activity and lipid accumulation in hepatocytes. Hepatocytes from WT mice were incubated in oleic acid-containing medium (600 μmol/L) with or without 100 nmol/L bortezomib (PS-341) for 48 hours, and subjected to Oil Red O staining and Western blot analysis. **A:** Representative photomicrographs of Oil Red O staining of hepatocytes. Scale bar = 50 μm. **B:** Lipids in hepatocytes were measured by digital image analysis. Data were corrected by cell numbers. $n = 10$ experiments/group. **C:** ADRP measured in hepatocytes treated with oleic acid and bortezomib. Data are expressed as means ± SD. $^{*}P < 0.05$ (Student's *t*-test).

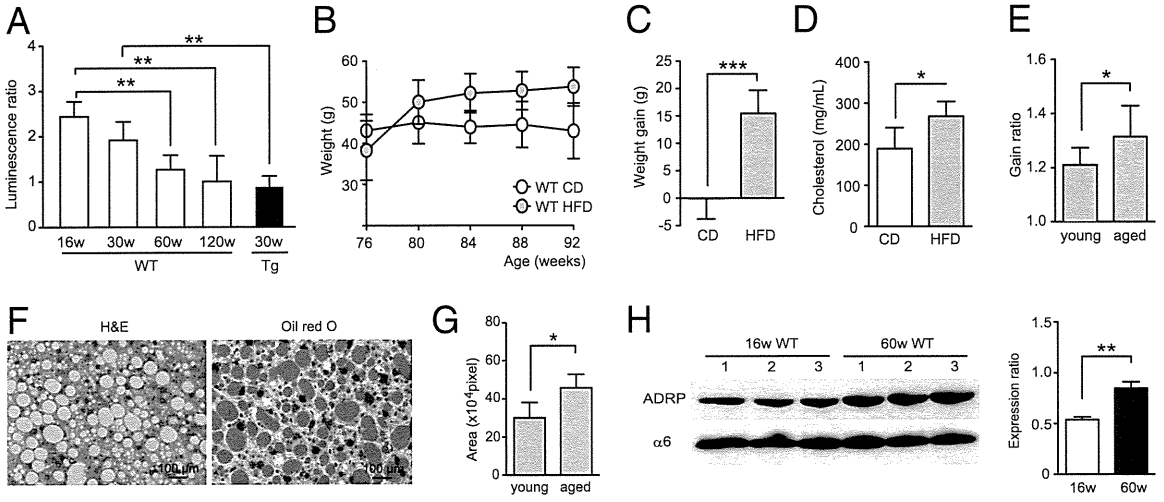

Figure 7. Steatosis and fat accumulation in HFD-fed aged WT mice. **A:** Proteasomal chymotrypsin-like activity in hepatocytes from WT and Tg mice. Isolated hepatocytes were subjected to luminescent assays using a specific luminogenic proteasome substrate, Suc-LLVY-aminoluciferin. The number of viable cells was measured by ATP assays using the luciferase reaction. Data are expressed as a Suc-LLVY luminescence/ATP luminescence ratio. n = 4, 5, or 6 mice per group. **B:** Body weight of aged CD- or HFD-fed WT mice. n = 4 or 5 mice per data point. **C:** Weight gain in CD- or HFD-fed WT mice between starting point (76 weeks old) and the endpoint (92 weeks old). n = 4 or 5 mice per group. **D:** Total blood cholesterol concentration (mg/mL) in CD- or HFD-fed WT mice. Data were measured at the endpoint (92 weeks old). n = 4 or 5 mice per group. **E:** Weight gain in young (22 weeks old) and aged (92 weeks old) WT mice after HFD feeding. Fold increase in body weight was calculated by dividing the body weight of HFD-fed mice by that of CD-fed mice. **F:** H&E and Oil Red O staining of liver sections from HFD-fed aged WT mice. Scale bars: 100 μm. **G:** Lipid accumulation in the liver of HFD-fed young (22 weeks old) and aged (92 weeks old) WT mice. n = 4 to 10 mice per group. **H:** Expression of ADRP in aged WT mice. Liver extracts from young (16 weeks old) and aged (60 weeks old) WT mice were immunoblotted with ADRP Ab (**left panel**). Lanes 1, 2, and 3 represent individual mice. The expression ratio of ADRP to proteasome subunit α6 was calculated (**right panel**). n = 3 mice per group. Data are expressed as means ± SD. *$P < 0.05$, **$P < 0.01$, and ***$P < 0.001$ (Student's t-test).

ADRP (Figures 4, 5, and 7). Thus, our results suggest that decreased proteasomal activity accelerates the aging process and promotes the development of age-related pathology.

Ub-conjugated substrates are known to accumulate in most aged tissues because of decreased removal by proteasomes.[22,23] However, little is known about the identity of specific substrate proteins that accumulate in the tissue of aged individuals. In the present study, using protein arrays we identified several proteins whose expression differed significantly between Tg and WT mice (Figure 3C and see Supplemental Table S1 at *http://ajp.amjpathol.org*). RNase L, whose expression was increased, is an effector molecule of the 2-5A system, a major enzymatic pathway regulated by interferons.[24,25] RNase L expression is increased in an age-dependent manner, and its ectopic expression induces a senescent morphology and accelerated replicative senescence in cultured cells.[25,26] Furthermore, RNase L knockout mice survive longer than RNase L WT mice.[27] On the other hand, Bcl-xL, whose expression was decreased in Tg mice, is an antiapoptotic protein that plays a central role in cell survival; it inhibits senescence induction in cultured cells by preventing generation of reactive oxygen species.[28] Thus, elevated expression of RNase L and decreased expression of Bcl-xL may be involved in the development of age-related phenotypes in Tg mice.

As in Tg mice, expression of RNase L was elevated in aged WT mice. In contrast, Bcl-xL expression was not significantly altered in aged mice (see Supplemental Figure S3 at *http://ajp.amjpathol.org*) whereas it was reduced in Tg mice. This discordance may be explained if reduction in proteasomal activity is more persistent and profound in Tg than in aged WT mice. Alternatively, substrate specificity of the proteasome may be altered by the incorporation of the β5t subunit. Bcl-xL is transcriptionally regulated by NF-κB, and activation and nuclear translocation of NF-κB are dependent on the degradation of inhibitory-κB (IκB) by proteasomes.[29] Incorporation of β5t may, for example, alter the substrate specificity of the proteasome so that IκB becomes more resistant to proteasomal degradation. Because altered substrate specificity of the proteasome should affect degradation of many other proteins, it may make a large contribution to the phenotypes of Tg mice, along with decreased chymotrypsin-like activity. In addition to RNase L and Bcl-xL, we identified several proteins that were differentially expressed in Tg and WT mice, but with no known functions in cellular senescence (see Supplemental Table S1 at *http://ajp.amjpathol.org*). Further studies of these proteins may provide new insights into the regulation of cellular senescence.

In addition to Ub-conjugated proteins, Tg mice accumulated oxidized proteins (Figure 3F). Oxidatively damaged proteins, which are normally removed by proteasomes,[30,31] are widely believed to contribute to the aging process.[31,32] Thus, the accumulation of oxidatively damaged proteins presumably constitutes an additional factor contributing to the age-related phenotype in Tg mice.

Many human diseases are age-related, and aging is known to increase the prevalence of metabolic disorders. Metabolic syndrome occurs more frequently in the elderly, and intake of high dietary fat has been shown to induce more fat accumulation in aged than in young individuals.[33–36] It has been assumed that altered physical activity and systemic metabolism, such as a reduction in systemic energy expenditure, are major risk factors for the development of metabolic disorders such as

obesity, hyperlipidemia, and liver steatosis. With the present study, we have provided *in vivo* and *in vitro* evidence linking decreased proteasomal activity and lipid accumulation. Our data suggest that, in addition to the aforementioned risk factors, an age-related decline in proteasomal activity is involved in the development of age-related metabolic disorders. Remarkably, HFD-fed aged WT mice developed more pronounced obesity and hepatic steatosis than young WT mice (Figure 7), suggesting that the metabolic abnormalities in Tg mice mimic those in aged mice. Specifically, ADRP expression was increased in the liver of both Tg and aged WT mice. ADRP is a constitutively expressed, lipid-droplet-associated protein that is rapidly degraded by proteasomes in the absence of lipids.[37–39] Its abundance is directly proportional to the amount of intracellular lipids, and its expression is increased in human diseases involving fat accumulation, such as hepatic steatosis.[40,41] Thus, upregulated expression of ADRP may in part account for the pronounced HFD-induced obesity and hepatic steatosis observed in Tg and aged WT mice.

In conclusion, the newly developed Tg model described here enabled us to address the *in vivo* significance of proteasomal chymotrypsin-like activity for the first time. Our results suggest that an age-related decline in proteasomal activity has an important role in the pathogenesis of age-related metabolic disorders and possibly in age-related disorders in general. Future studies are needed to address the molecular mechanisms underlying an age-related decrease in proteasomal activity and to identify specific substrate proteins, the altered expression of which is involved in the development of age-related diseases. Such studies may provide a new approach to the prevention and treatment of age-related diseases.

Acknowledgments

We thank Chisato Sudo, Saori Konno, Yuki Matsui, and Dr. Mitsufumi Nishio (Hokkaido University Graduate School of Medicine) for technical support and the staff of the Institute for Animal Experimentation (Hokkaido University Graduate School of Medicine) for mouse maintenance.

References

1. Ciechanover A: Proteolysis: from the lysosome to ubiquitin and the proteasome. Nat Rev Mol Cell Biol 2005, 6:79–87
2. Coux O, Tanaka K, Goldberg AL: Structure and functions of the 20S and 26S proteasomes. Annu Rev Biochem 1996, 65:801–847
3. Kloetzel PM: The proteasome and MHC class I antigen processing. Biochim Biophys Acta 2004, 1695:225–233
4. Baumeister W, Walz J, Zühl F, Seemüller E: The proteasome: paradigm of a self-compartmentalizing protease. Cell 1998, 92:367–380
5. Kisselev AF, Callard A, Goldberg AL: Importance of the different proteolytic sites of the proteasome and the efficacy of inhibitors varies with the protein substrate. J Biol Chem 2006, 281:8582–8590
6. Ludwig H, Khayat D, Giaccone G, Facon T: Proteasome inhibition and its clinical prospects in the treatment of hematologic and solid malignancies. Cancer 2005, 104:1794–1807
7. Voorhees PM, Dees EC, O'Neil B, Orlowski RZ: The proteasome as a target for cancer therapy. Clin Cancer Res 2003, 9:6316–6325
8. Gaczynska M, Osmulski PA, Ward WF: Caretaker or undertaker? The role of the proteasome in aging. Mech Ageing Dev 2001, 122:235–254
9. Chondrogianni N, Gonos ES: Proteasome dysfunction in mammalian aging: steps and factors involved. Exp Gerontol 2005, 40:931–938
10. Dahlmann B: Role of proteasomes in disease. BMC Biochem 2007, 8 Suppl 1:S3
11. Tonoki A, Kuranaga E, Tomioka T, Hamazaki J, Murata S, Tanaka K, Miura M: Genetic evidence linking age-dependent attenuation of the 26S proteasome with the aging process. Mol Cell Biol 2009, 29:1095–1106
12. Sasaki K, Hamazaki J, Koike M, Hirano Y, Komatsu M, Uchiyama Y, Tanaka K, Murata S: PAC1 gene knockout reveals an essential role of chaperone-mediated 20S proteasome biogenesis and latent 20S proteasomes in cellular homeostasis. Mol Cell Biol 2010, 30:3864–3874
13. Murata S, Sasaki K, Kishimoto T, Niwa S, Hayashi H, Takahama Y, Tanaka K: Regulation of CD8+ T cell development by thymus-specific proteasomes. Science 2007, 316:1349–1353
14. Tomaru U, Ishizu A, Murata S, Miyatake Y, Suzuki S, Takahashi S, Kazamaki T, Ohara J, Baba T, Iwasaki S, Fugo K, Otsuka N, Tanaka K, Kasahara M: Exclusive expression of proteasome subunit β5t in the human thymic cortex. Blood 2009, 113:5186–5191
15. Nitta T, Murata S, Sasaki K, Fujii H, Ripen AM, Ishimaru N, Koyasu S, Tanaka K, Takahama Y: Thymoproteasome shapes immunocompetent repertoire of CD8+ T cells. Immunity 2010, 32:29–40
16. Murata S, Yashiroda H, Tanaka K: Molecular mechanisms of proteasome assembly. Nat Rev Mol Cell Biol 2009, 10:104–115
17. Niwa H, Yamamura K, Miyazaki J: Efficient selection for high-expression transfectants with a novel eukaryotic vector. Gene 1991, 108:193–199
18. Levine RL, Garland D, Oliver CN, Amici A, Climent I, Lenz AG, Ahn BW, Shaltiel S, Stadtman ER: Determination of carbonyl content in oxidatively modified proteins. Methods Enzymol 1990, 186:464–478
19. Levine RL, Williams JA, Stadtman ER, Shacter E: Carbonyl assays for determination of oxidatively modified proteins. Methods Enzymol 1994, 233:346–357
20. Gong J, Sun Z, Li P: CIDE proteins and metabolic disorders. Curr Opin Lipidol 2009, 20:121–126
21. Miura S, Gan JW, Brzostowski J, Parisi MJ, Schultz CJ, Londos C, Oliver B, Kimmel AR: Functional conservation for lipid storage droplet association among Perilipin, ADRP, and TIP47 (PAT)-related proteins in mammals, Drosophila, and Dictyostelium. J Biol Chem 2002, 277:32253–32257
22. Carrard G, Bulteau AL, Petropoulos I, Friguet B: Impairment of proteasome structure and function in aging. Int J Biochem Cell Biol 2002, 34:1461–1474
23. Ciechanover A, Orian A, Schwartz AL: The ubiquitin-mediated proteolytic pathway: mode of action and clinical implications. J Cell Biochem Suppl 2000, 34:40–51
24. Zhou A, Hassel BA, Silverman RH: Expression cloning of 2-5A-dependent RNAase: a uniquely regulated mediator of interferon action. Cell 1993, 72:753–765
25. Bisbal C, Silverman RH: Diverse functions of RNase L and implications in pathology. Biochimie 2007, 89:789–798
26. Floyd-Smith G, Denton JS: Age-dependent changes are observed in the levels of an enzyme mediator of interferon action: a (2′-5′)A(n)-dependent endoribonuclease. Proc Soc Exp Biol Med 1988, 189:329–337
27. Andersen JB, Li XL, Judge CS, Zhou A, Jha BK, Shelby S, Zhou L, Silverman RH, Hassel BA: Role of 2-5A-dependent RNase-L in senescence and longevity. Oncogene 2007, 26:3081–3088
28. Jung MS, Jin DH, Chae HD, Kang S, Kim SC, Bang YJ, Choi TS, Choi KS, Shin DY: Bcl-xL and E1B-19K proteins inhibit p53-induced irreversible growth arrest and senescence by preventing reactive oxygen species-dependent p38 activation. J Biol Chem 2004, 279:17765–17771
29. Fennell DA, Chacko A, Mutti L: BCL-2 family regulation by the 20S proteasome inhibitor bortezomib. Oncogene 2008, 27:1189–1197
30. Friguet B, Bulteau AL, Chondrogianni N, Conconi M, Petropoulos I: Protein degradation by the proteasome and its implications in aging. Ann N Y Acad Sci 2000, 908:143–154
31. Grimm S, Höhn A, Grune T: Oxidative protein damage and the proteasome. Amino Acids 2012, 42:23–38

32. Johnson FB, Sinclair DA, Guarente L: Molecular biology of aging. Cell 1999, 96:291–302
33. Denys K, Cankurtaran M, Janssens W, Petrovic M: Metabolic syndrome in the elderly: an overview of the evidence. Acta Clin Belg 2009, 64:23–34
34. Zamboni M, Mazzali G, Zoico E, Harris TB, Meigs JB, Di Francesco V, Fantin F, Bissoli L, Bosello O: Health consequences of obesity in the elderly: a review of four unresolved questions. Int J Obes (Lond) 2005, 29:1011–1029
35. Nishikawa S, Yasoshima A, Doi K, Nakayama H, Uetsuka K: Involvement of sex, strain and age factors in high fat diet-induced obesity in C57BL/6J and BALB/cA mice. Exp Anim 2007, 56:263–272
36. Hoffler U, Hobbie K, Wilson R, Bai R, Rahman A, Malarkey D, Travlos G, Ghanayem BI: Diet-induced obesity is associated with hyperleptinemia, hyperinsulinemia, hepatic steatosis, and glomerulopathy in C57Bl/6J mice. Endocrine 2009, 36:311–325
37. Brasaemle DL, Barber T, Wolins NE, Serrero G, Blanchette-Mackie EJ, Londos C: Adipose differentiation-related protein is an ubiquitously expressed lipid storage droplet-associated protein. J Lipid Res 1997, 38:2249–2263
38. Masuda Y, Itabe H, Odaki M, Hama K, Fujimoto Y, Mori M, Sasabe N, Aoki J, Arai H, Takano T: ADRP/adipophilin is degraded through the proteasome-dependent pathway during regression of lipid-storing cells. J Lipid Res 2006, 47:87–98
39. Xu G, Sztalryd C, Lu X, Tansey JT, Gan J, Dorward H, Kimmel AR, Londos C: Post-translational regulation of adipose differentiation-related protein by the ubiquitin/proteasome pathway. J Biol Chem 2005, 280:42841–42847
40. Heid HW, Moll R, Schwetlick I, Rackwitz HR, Keenan TW: Adipophilin is a specific marker of lipid accumulation in diverse cell types and diseases. Cell Tissue Res 1998, 294:309–321
41. Motomura W, Inoue M, Ohtake T, Takahashi N, Nagamine M, Tanno S, Kohgo Y, Okumura T: Up-regulation of ADRP in fatty liver in human and liver steatosis in mice fed with high fat diet. Biochem Biophys Res Commun 2006, 340:1111–1118

Viruses **2011**, *3*, 1532-1548; doi:10.3390/v3091532

OPEN ACCESS

viruses

ISSN 1999-4915

www.mdpi.com/journal/viruses

Review

Human T-Lymphotropic Virus Type 1 (HTLV-1) and Regulatory T Cells in HTLV-1-Associated Neuroinflammatory Disease

Natsumi Araya [1], Tomoo Sato [1], Naoko Yagishita [1], Hitoshi Ando [1], Atae Utsunomiya [2], Steven Jacobson [3] and Yoshihisa Yamano [1,*]

[1] Department of Rare Diseases Research, Institute of Medical Science, School of Medicine, St. Marianna University, Kawasaki 216-8511, Japan; E-Mails: araya@marianna-u.ac.jp (N.A.); tomoo@marianna-u.ac.jp (T.S.); yagi@marianna-u.ac.jp (N.Y.); hando@marianna-u.ac.jp (H.A.)

[2] Department of Hematology, Imamura Bun-in Hospital, Kagoshima 890-0064, Japan; E-Mail: autsunomiya@jiaikai.jp

[3] Viral Immunology Section, Neuroimmunology Branch, National Institute of Neurological Disorders and Stroke, National Institutes of Health, Bethesda, MD 20892, USA; E-Mail: jacobsons@ninds.nih.gov

* Author to whom correspondence should be addressed; E-Mail: yyamano@marianna-u.ac.jp; Tel.: +81-44-977-8111; Fax: +81-44-977-9772.

Received: 2 June 2011; in revised form: 13 August 2011 / Accepted: 16 August 2011 / Published: 25 August 2011

Abstract: Human T-lymphotropic virus type 1 (HTLV-1) is a retrovirus that is the causative agent of adult T cell leukemia/lymphoma (ATL) and associated with multiorgan inflammatory disorders, including HTLV-1-associated myelopathy/tropical spastic paraparesis (HAM/TSP) and uveitis. HTLV-1-infected T cells have been hypothesized to contribute to the development of these disorders, although the precise mechanisms are not well understood. HTLV-1 primarily infects $CD4^+$ T helper (Th) cells that play a central role in adaptive immune responses. Based on their functions, patterns of cytokine secretion, and expression of specific transcription factors and chemokine receptors, Th cells that are differentiated from naïve $CD4^+$ T cells are classified into four major lineages: Th1, Th2, Th17, and T regulatory (Treg) cells. The $CD4^+CD25^+CCR4^+$ T cell population, which consists primarily of suppressive T cell subsets, such as the Treg and Th2 subsets in healthy individuals, is the predominant viral reservoir of HTLV-1 in both ATL and HAM/TSP patients. Interestingly, $CD4^+CD25^+CCR4^+$ T cells become Th1-like cells in

HAM/TSP patients, as evidenced by their overproduction of IFN-γ, suggesting that HTLV-1 may intracellularly induce T cell plasticity from Treg to IFN-γ^+ T cells. This review examines the recent research into the association between HTLV-1 and Treg cells that has greatly enhanced understanding of the pathogenic mechanisms underlying immune dysregulation in HTLV-1-associated neuroinflammatory disease.

Keywords: HTLV-1; HAM/TSP; ATL; $CD4^+CD25^+CCR4^+$ T cell; regulatory T cell; ex$Foxp3^+$ cell; inflammation; immune-dysfunction

1. Introduction

Human T-lymphotropic virus type 1 (HTLV-1) is a retrovirus associated with chronic, persistent infection of human T cells. HTLV-1 infection is endemic in Japan, the Caribbean, and part of South America, Africa, the Middle East, and Melanesia [1]. Studies conducted in HTLV-1 endemic areas have demonstrated that HTLV-1 infection is associated with a variety of human diseases, including an aggressive mature T cell malignancy termed adult T-cell leukemia (ATL) [2], which is defined as neoplastic growth of HTLV-1-infected T cells. HTLV-1 is also associated with non-neoplastic inflammatory conditions such as HTLV-1-associated myelopathy/tropical spastic paraparesis (HAM/TSP) [3,4], uveitis [5], Sjögren syndrome [6], bronchoalveolitis, arthritis [7], and polymyositis [8], where high tissue concentrations of HTLV-1 infected T lymphocytes have been observed. Importantly, some patients have more than one of these HTLV-1-associated inflammatory conditions [9].

Although HTLV-1-associated disorders have been extensively studied, the exact mechanism by which HTLV-1 induces these inflammatory conditions is not completely understood. The proviral load of HTLV-1 may contribute to development of HTLV-1-associated inflammatory conditions, since the number of HTLV-1-infected T cells circulating in the peripheral blood is higher in patients with HAM/TSP than in asymptomatic HTLV-1-infected individuals [10,11], and is even higher in the cerebrospinal fluid of patients with HAM/TSP [12]. In HAM/TSP patients, the proviral load correlates with not only the percentage of activated $CD4^+$ T cells but also with that of HTLV-1-specific $CD8^+$ cytotoxic T lymphocytes (CTLs) [11,13]. These HTLV-1-specific CTLs produce various cytokines, such as IFN-γ and TNF-α, that may suppress viral replication and kill infected cells and/or promote bystander activation and killing of nearby resident cells in the central nervous system (CNS) [14–17]. In addition, increased viral expression, particularly of the transactivating viral gene encoding HTLV-1 Tax, has also been hypothesized to play a role in HTLV-1 disease progression [11,12]. Transgenic mice expressing HTLV-1 Tax develop an inflammatory arthropathy [18], and transgenic rats expressing HTLV-1 env-pX develop destructive arthropathy, Sjögren syndrome, vasculitis, and polymyositis [19]. These findings support the hypothesis that HTLV-1 *tax* is one of the exogenous retrovirus genes responsible for immune dysregulation.

HTLV-1 Tax is a transactivator/oncoprotein that has potent effects on infected T cells, including activation of nuclear factor(NF)-κB [20] with subsequent enhancement of cell activation and proliferation and expression of various cellular genes, such as IL-2 [21], the α-chain of the IL-2 receptor (IL-2Rα) [22], IL-15 [23], and IL-15Rα [24]. Such virus-induced intracellular activation may

directly contributes to T cell activation and the *ex vivo* T cell proliferation observed in patients with HAM/TSP [25]. These findings suggest that invasion by HTLV-1-infected T cells, together with viral gene expression and cellular-signaling mechanisms, trigger a strong virus-specific immune response and increased proinflammatory cytokine production, leading to CNS inflammation and autologous tissue damage. However, the precise mechanisms underlying the induction of immune activation by HTLV-1-infected T cells are not well understood.

2. HTLV-1 and Regulatory T Cells

The recent discovery of regulatory T cells (Treg cells) has generated new opportunities for and increased interest in elucidating the above mentioned mechanisms. In healthy individuals, the Treg cells, a subset of $CD4^+CD25^+$ T cells, play a key role in maintaining immune system homeostasis by suppressing the proliferation of and cytokine production by pathogenic T cells [26]. Although Treg cells are phenotypically similar to activated T cells, they can be identified *ex vivo* by their intracellular expression of the transcriptional regulator Foxp3 [27], which is critical in the development and functioning of Treg cells in both mice and humans. Significant reductions in Foxp3 expression and/or Treg cell function have been observed in patients with several types of human autoimmune diseases [28], suggesting that defects in Foxp3 expression and/or Treg functioning may precipitate loss of immunological tolerance. $CD4^+CD25^+$ T cells are also the predominant viral reservoir in the peripheral blood of HTLV-1-infected individuals [29]. Recently, significant reductions in Foxp3 expression and Treg cell function have been observed in $CD4^+CD25^+$ T cells from patients with HAM/TSP [30–34]. Furthermore, decreased expression levels of CTL antigen-4 (CTLA-4), a Treg-associated immune-suppressive molecule, and glucocorticoid-induced tumor necrosis factor receptor-related protein (GITR) have also been observed on the $CD4^+CD25^+$ T cells of HAM/TSP patients [30,34]. Notably, overexpression of HTLV-1 Tax has been observed to reduce Foxp3 expression and inhibit the suppressive function of Treg cells *in vitro* [30]. Furthermore, because of a Tax-induced defect in TGF-β signaling, Foxp3 expression was decreased and Treg functions were impaired in patients with HAM/TSP [35]. Recently, significantly decreased numbers of $CD4^+CD25^+Foxp3^+$ Treg cells were observed in transgenic mice expressing HTLV-1 Tax that develop an inflammatory arthropathy [36]. In addition, increased viral expression of the HTLV-1 bZIP factor (*HBZ*) gene encoding the minus strand of HTLV-1 has also been suggested to play a role in HTLV-1 disease progression [37], and $CD4^+Foxp3^+$ Treg cells in HBZ transgenic mice were functionally impaired [38]. These findings indicate that HTLV-1-induced dysfunctioning of $CD4^+CD25^+$ Treg cells may be one of the mechanisms underlying the induction of immune activation by HTLV-1-infected T cells.

In contrast to the decreased expression of Foxp3 in $CD4^+CD25^+$ T cells observed in HAM/TSP patients [30–34], most $CD4^+CD25^+$ ATL cells have been shown to express Foxp3 in patients with ATL [39,40]. Therefore, it has been hypothesized that ATL cells may be derived from Treg cells [41]. Interestingly, some ATL cells exhibit immunosuppressive functions similar to those of Treg cells, which may contribute to clinically observed cellular immunodeficiency in ATL patients [41–43], although some of these ATL cells lose this regulatory function [44].

3. HTLV-1 and $CD4^+CD25^+CCR4^+$ T Cells

Although HTLV-1 has been reported to infect a number of cell types both *in vitro* and *in vivo* [29,45–49], $CD4^+$ Th cells, which play a central role in adaptive immune responses, are the predominant viral reservoir in the peripheral blood [50]. To understand the effects of HTLV-1 infection on the functioning of $CD4^+$ Th cells, it is necessary to discover if, and if so which of the Th subpopulations is preferentially infected with HTLV-1. Based on their functions, patterns of cytokine secretion, and expression of specific transcription factors and chemokine receptors, $CD4^+$ Th cells, which are differentiated from naïve $CD4^+$ T cells, are classified into four major lineages: Th1, Th2, Th17, and Treg cells (Figure 1).

Figure 1. T cell subsets of $CD4^+$ T helper cells. Th cells are differentiated from naïve $CD4^+$ T cells into 4 major lineages: Th1, Th2, Th17, and T-regulatory (Treg) cells. Each Th subset exhibits characteristic functions, patterns of cytokine secretion, and expression of specific chemokine receptors.

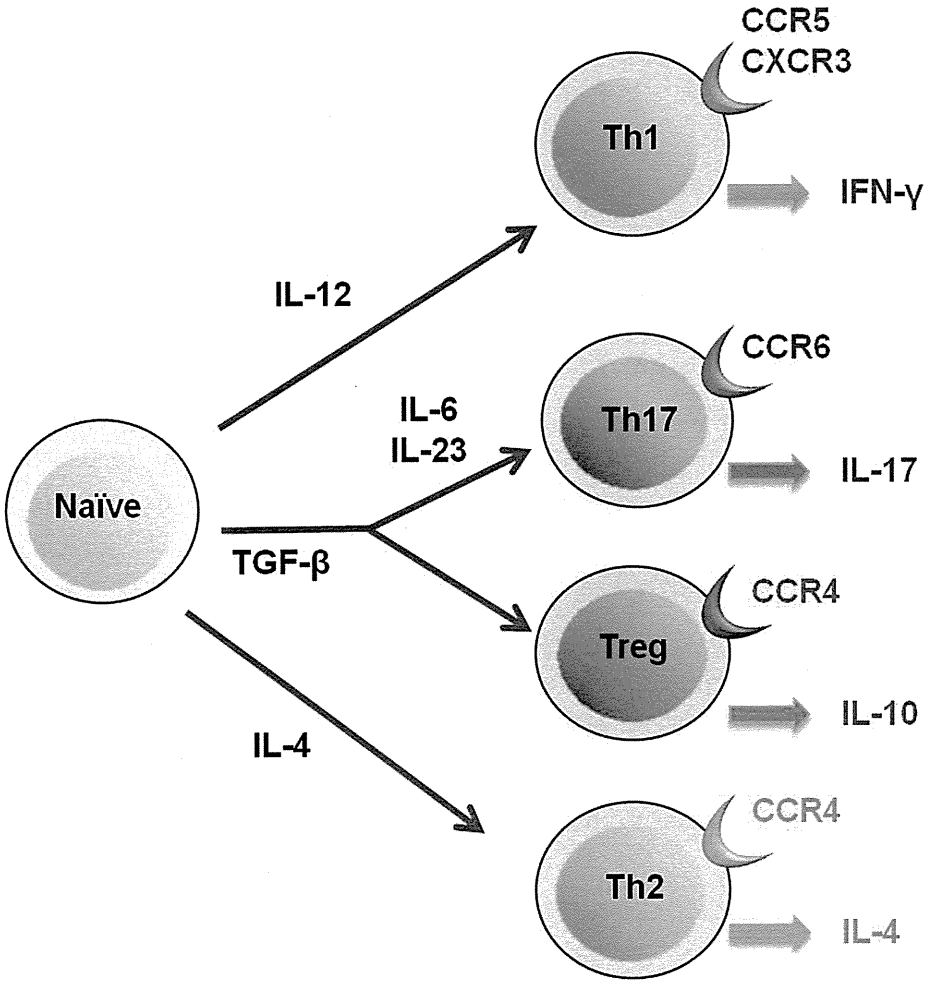

The chemokine receptor CCR4 has recently been found to be expressed on HTLV-1-infected leukemia cells in ATL patients [51]. Because CCR4 is known to be selectively expressed on Treg and Th2 cells [51–53] (Figure 1) and because most ATL cells express high levels of Foxp3, it has been hypothesized that ATL cells may be derived from Treg cells [41]. Although it has been

demonstrated that $CD4^+CD25^+$ T cells in HAM/TSP patients exhibit reduced Foxp3 expression and Treg suppression [30–33] and that HTLV-1-infected $CD4^+$ T cells in HAM/TSP patients produce Th1 cytokines (IFN-γ) [16,30], it has also been observed that CCR4 selectively overexpresses on HTLV-1-infected T cells in HAM/TSP patients [54]. Furthermore, the majority of $CD4^+CD25^+CCR4^+$ T cells have been found to be infected with HTLV-1 and this T cell subset has increased numbers in HAM/TSP patients [54]. Thus, $CD4^+CD25^+CCR4^+$ T cells are a major reservoir of HTLV-1-infected T cells, which are increased in numbers in both HAM/TSP and ATL patients.

4. HTLV-1 and $Foxp3^-CD4^+CD25^+CCR4^+$ T Cells

Although CCR4 is known to be selectively expressed on Treg and Th2 cells in healthy individuals, more detailed flow cytometric analysis of Foxp3 expression in $CD4^+CD25^+CCR4^+$ T cells of HAM/TSP patients demonstrated that the frequency of the $Foxp3^-$ population was greatly increased in $CD4^+CD25^+CCR4^+$ T cells [54]. Moreover, analysis of proinflammatory cytokine expression in this $Foxp3^-CD4^+CD25^+CCR4^+$ T cell subset demonstrated that these cells uniquely produced multiple proinflammatory cytokines such as IL-2, IL-17, and few IFN-γ in healthy individuals while $Foxp3^+CD4^+CD25^+CCR4^+$ T cells (Treg cells) did not. Furthermore, it was demonstrated that HAM/TSP patients had only few $Foxp3^+CD4^+CD25^+CCR4^+$ T cells that did not produce such cytokines [54]. The $Foxp3^-CD4^+CD25^+CCR4^+$ T cells in HAM/TSP were greater in number and overproduced IFN-γ [54]. Further, the proportion of these IFN-γ-producing $Foxp3^-CD4^+CD25^+CCR4^+$ T cells may have a functional consequence, since the presence of this subpopulation could be correlated with disease activity and severity of HAM/TSP *in vivo* [54]. Thus, in a $CD4^+CD25^+CCR4^+$ T cell population that mainly consists of suppressive T cell subsets such as Treg and Th2 under healthy conditions, IFN-γ-producing $Foxp3^-CD4^+CD25^+CCR4^+$ T cells, rarely encountered in healthy individuals, were increased in number and overproduced IFN-γ in HAM/TSP patients (Figure 2). We therefore propose to call this IFN-$\gamma^+Foxp3^-CD4^+CD25^+CCR4^+$ T cell subset T_{HAM} cells. Interestingly, increased numbers of $Foxp3^{low}CD4^+CD25^+$ memory T cells, which have cytokine secretion patterns similar to those of T_{HAM} cells, have recently been observed in patients with active systemic lupus erythematosus (SLE) [55]. Therefore, it would be of interest to build on this finding by confirming whether this newly defined unique T cell subset, which has been observed in both HAM/TSP and SLE patients, is found in both these patient groups and can be functionally deregulated in other immunological diseases.

Although most $CD4^+CD25^+CCR4^+$ T cells are infected with HTLV-1 in both HAM/TSP and ATL patients [54,56], the ratio of T_{HAM} cells ($CCR4^+Foxp3^-$ with IFN-γ production) to Treg cells ($CCR4^+Foxp3^+$ with no cytokine production) in the $CD4^+CD25^+CCR4^+$ T cell subset has been found to be high in HAM/TSP patients but low in ATL patients [54]. This differential T_{HAM}/Treg ratio in HTLV-1-infected T cells may be associated with the differential immune responses observed between HAM/TSP and ATL patients (Figure 3). ATL patients tend to have very low numbers of Tax-specific $CD8^+$ T cells in peripheral blood mononuclear cells (PBMCs) and to develop opportunistic infections [57,58], while HAM/TSP patients tend to have high numbers of Tax-specific $CD8^+$ CTLs [11,12,14,59]. As $CD4^+CD25^+$ T cells with high levels of Foxp3 expression have been reported to have an immunosuppressive function in ATL patients [41–43], the increased number of

$CD4^+CD25^+CCR4^+$ leukemia T cells with Treg functions observed in ATL patients may contribute to their clinically observed cellular immunodeficiency. However, HAM/TSP patients show very high cellular and humoral immune responses, such as high proportions of Tax-specific $CD8^+$ T cells, as well as cytomegalovirus (CMV)-specific $CD8^+$ T cells in the PBMCs [14,33]; high antibody titer to HTLV-1 [9]; and increased production of proinflammatory cytokines, such as IL-12 and IFN-γ [60]. It has been reported that $CD4^+CD25^+$ T cells with low expression of Foxp3 [30] and HTLV-1 Tax-expressing $Foxp3^+$ Treg cells [61] extracted from HAM/TSP patients exhibit defective immunosuppressive functioning. Moreover, it has been demonstrated that HTLV-1-infected IFN-γ-overproducing $CD4^+CD25^+CCR4^+Foxp3^-$ T cells (T_{HAM} cells) increase in number in HAM/TSP patients, and their levels can be correlated with disease severity [54]. Thus, $CD4^+CD25^+CCR4^+$ T cells with increased proinflammatory functioning, together with a defective Treg compartment [30–33,54], may overcome the regulatory effect of HTLV-1-uninfected Treg cells [61] and at least partly account for the heightened immune response observed in HAM/TSP patients. Collectively, these observations support the hypothesis that an imbalance in the T_{HAM}/Treg ratio in HTLV-1-infected $CD4^+CD25^+CCR4^+$ T cells is an important contributing factor in the immunological differences in host immune response observed between HAM/TSP and ATL patients (Figure 3).

Figure 2. Cellular components of $CD4^+CD25^+CCR4^+$ T cells in healthy donors and HAM/TSP patients. In healthy donors, the $CD4^+CD25^+CCR4^+$ T cell population primarily consists of suppressive T cell subsets, such as Treg and Th2, whereas that of HTLV-1-associated myelopathy/tropical spastic paraparesis (HAM/TSP) patients consists of an increased number of IFN-γ-producing $Foxp3^-CD4^+CD25^+CCR4^+$ T cells (T_{HAM} cells).